https://doi.org/10.5194/nhess-2023-166
Preprint. Discussion started: 18 October 2023

Natural Hazards and Earth System Sciences
Discussions

Control of erosion damage of the hinterland by due to construction of submerged detached breakwater

Changbin Lim[1,2], Jinhoon Kim[3], Jong-Beom Kim[4], and Jung-Lyul Lee[2,5]

[1]Environmental Hydraulics Institute, Universidad de Cantabria – Avda. Isabel Torres, 15, Parque Cientìfico y Technològico de Cantabria, 39011, Santander, Spain
[2]School of Civil, Architecture and Environmental System Engineering, Sungkyunkwan University, Suwon, 16419, Republic of Korea
[3]Department of Earth and Environmental Engineering Kangwon National University, Samcheok, 25913, Republic of Korea
[4]Department of Coastal Management, GeoSystem Research Corporation, Gunpo, 15807, Republic of Korea
[5]Graduate School of Water Resources, Sungkyunkwan University, Suwon, 16419, Republic of Korea

Correspondence to: Jung-Lyul Lee (jllee6359@hanmail.net)

Abstract. Submerged detached breakwaters (SDBWs) have increasingly been used in recent times as an alternative against their emergent counterpart (EDBWs) to mitigate erosion because the former do not spoil the seascape. Both of these structures are (usually) constructed using precast concrete blocks or natural granite rocks, hence becoming permeable structures. In the case of a single EDBW, a parabolic bay shape equation can be readily used to assess the shoreline planform behind the structure, yet no direct method for the SDBW. In this study, the variation in the initial curved equilibrium planform downdrift of a harbor breakwater, before and after the installation of SDBWs, is estimated by the wave transmission coefficient through an SDBW and calculated longshore sediment transport of which the wave diffraction is considered. This is to say that the shore-normal direction varies (rotates) along a curved equilibrium planform. The applicability of this methodology is validated by comparing the observed data (wave and shoreline change) using closed circuit television on Bongpo-Cheonjin Beach in South Korea, with the calculated shoreline changes. This rational approach, though with some limitations, for shoreline change behind permeable SDBWs will benefit the work on coastal management and mitigation of beach erosion.

1. Introduction

Historically, coasts were used mainly for fishing and playing on the beach. Nowadays, it has become a popular place for recreational activities, such as swimming, surfing, scuba diving, and windsurfing, as well as a destination for tourists. For these reasons, coastal structures are important to protect a beach for local economic growth. However, while the protective structures are favorable, they have often adversely caused beach erosion, in addition to reckless development projects and climate change that may have contributed to accelerating beach erosion. Therefore, diverse countermeasures should be provided to reduce beach erosion (Lim et al., 2021b).

https://doi.org/10.5194/nhess-2023-166
Preprint. Discussion started: 18 October 2023


Natural Hazards and Earth System Sciences Discussions

Recently, submerged detached breakwaters (SDBWs) have been constructed instead of emergent detached breakwaters (EDBWs) to mitigate beach erosion, to conserve the beach landscape. Thus, a critical requirement has arisen for researching how these structures affect shoreline changes. In this paper, permeable SDBWs that can partially reflect and transmit waves are tentatively referred to as permeable structures to ease the task of analysis.

Coastal structures, such as SDBWs and EDBWs, are built to reduce incident wave energy and to protect the beach from wave action. Theoretically, Wang et al. (1975) proposed the shoreline response (i.e., advance or retreat) caused by incident waves. Yates et al. (2009) conducted long-term field observations to obtain a general understanding of incident wave energy that affects shoreline advance or retreat at mean sea level. This work has been extended to estimate the location affected by incident wave energy (Kim et al., 2021; Lim et al., 2022c).

For example, Kim et al. (2021) proposed a bulk-type model that can predict the affected shoreline position by applying the results of Yates et al. (2009). Thus, arranging coastal structures, including SDBW or EDBW, to control storm waves, can reduce incident wave energy behind the structures and episodic shoreline retreat. This approach disregards the impacts induced by the longshore sediment transport rate (LSTR). Depending on the magnitude of the LSTR, shoreline changes can be managed accordingly (Kim and Lee, 2018; Kim et al., 2021). Although SDBWs or EDBWs are favorable for reducing storm wave energy to the beach, they often cause adverse effects on the shoreline as bay shape forms due to wave diffraction around the structures that change the wave hydrodynamic characteristics (i.e., wave height and wave direction). This produces phase difference and generates longshore sediment transport (LSTR) heading towards the lee of each structure (Lim et al., 2021a). Consequently, it may result in salient or tombolo planform in the lee of each structure unit, accompanied by erosion between two consecutive units and a reduction in incident wave height.

Without continuous sediment supply from upcoast or other littoral cells, erosion could occur at the nearby beach away from the structures. Thus, research is required to investigate the effect of constructing SDBW or EDBW on sandy shorelines. In this study, a typical case is reported to explain the effect of SDBWs installed at the center of Yeongrang Beach in South Korea, aiming to reduce erosion damage caused by the construction of artificial headland, which was fruitless due to the lack of understanding of the functions of the structure (Kang et al., 2010; Lim et al., 2019).

On the contrary, a significant amount of research publications are available on static equilibrium planform (SEP) resulting from the construction of impermeable structures such as EDBW (Inman and Frautschy, 1966; Noble, 1978; Gourlay, 1981; Nir, 1982; Dally and Pope, 1986; Suh and Dalrymple, 1987; Herbich, 1989; Hsu and Silvester, 1990; Ahrens and Cox, 1990; McCormick, 1993). Hanson and Kraus (1989) also used a long-term shoreline change model to perform numerical modeling for a beach that has impermeable breakwaters in place. Wamsley et al. (2002) used a numerical model to study shoreline responses behind EDBWs. Recently, Lim et al. (2021a) proposed a model of shoreline changes behind impermeable structures by applying the parabolic bay shape equation (PBSE; Hsu and Evans, 1989).

Although many laboratory experiments have been conducted to examine the three-dimensional phenomenon of current and sedimentation characteristics in the vicinity of coastal structures our understanding remains inadequate even for topographic changes associated with SDBWs (Hur, 2004; Lee et al., 2009; Newman, 1965; Kobayashi and Wurjanto, 1989; van der Meer

https://doi.org/10.5194/nhess-2023-166
Preprint. Discussion started: 18 October 2023


Natural Hazards and Earth System Sciences Discussions

and Deamen, 1994). Therefore, further study is needed to scrutinize the design details (cross-section and degree of submergence) and to clarify the likely impacts of shoreline change caused by constructing the SDBWs.

The main purpose of this study is to examine how much wave energy reduction is provided by the transmission rate of an SDBW and what impact the diffraction process on the SEP behind the structure and the LSTR. Furthermore, the study intends to validate the theoretical analysis by comparing its prediction with the field data observed obtained by a closed circuit television (CCTV) system on the east coast of South Korea.

In this paper, the PBSE, an empirical formula proposed by Hsu and Evans (1989), is briefly presented to predict the SEP due to the construction of EDBW in Section 2. Impacts of SDBW on SEP are predicted using the LSTR formula including wave transmission coefficient and wave diffraction in Section 3. In Section 4, the application of the methodology proposed in this study is conducted at Bongpo-Cheonjin Beach on the east coast of South Korea, where four SDBWs and one groin were constructed after downdrift beach erosion occurred due to a long breakwater for the harbor. Applying long-term wave observation data in deep water, transmission coefficient K_t are calibrated and applied to estimate the longshore sediment transport for calculation of the shoreline change behind the coastal structures. Discussions including shortcomings are stated in Section 5, with conclusions presented in Section 6.

2. Static equilibrium due to construction of emerged detached breakwater

2.1 Parabolic bay shape equation (PBSE)

The parabolic bay shape equation (PBSE) given by Hsu and Evans (1989) is applied to predict the static equilibrium planform resulting from the construction of an EDBW (Fig. 1),

$$R_n = \frac{a}{\sin\beta}[C_0 + C_1(\beta/\theta_n) + C_2(\beta/\theta_n)^2] \quad \text{for } \theta_n \geq \beta \tag{1a}$$

$$R_n = \frac{a}{\sin\theta_n} \quad \text{for } \theta_n < \beta \tag{1b}$$

where R_n is the radial distance from the focus to a point P on the static planform, θ_n is the angle between the wave crest baseline and the line joining the focus, and point P, a is the vertical distance between the wave crest baseline and the shore baseline passing through the downcoast control point Q, while β is the reference wave angle between the wave crest baseline at the focus and the control line R_n linking point Q and the focus, According to Hsu and Evans (1989), coefficients C_i ($i = 1, 2, 3$) are a function of β for best-fit the static equilibrium planform. The sum of these three coefficients is unity (one) at downcoast control point Q (Tan and Chiew, 1993). At point Q, the predominant wave direction is assumed to be in perpendicular to the shore baseline.

https://doi.org/10.5194/nhess-2023-166
Preprint. Discussion started: 18 October 2023

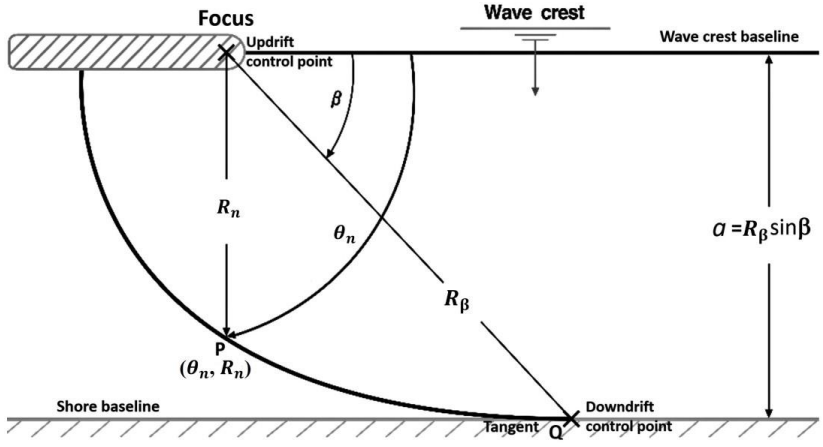

Figure 1: Definition sketch of parabolic bay shape equation.

Nowadays, the PBSE is the most used model for predicting the SEP in coastal engineering and management (USACE, 2002; Herrington et al., 2007; Bowman et al., 2009; Silveira et al., 2010; Yu and Chen, 2011; Anh et al., 2015; Thomas et al., 2016; and Ab Razak et al., 2018a & 2018b), despite the uncertainty reported by some users in locating the downcoast control point (Lausman et al., 2010a & 2010b). Recently, Lim et al. (2022a) clarified the uncertainty by recasting the PBSE using polar coordinates.

2.2 Validity of parabolic model

The parabolic model, implying the application of the PBSE, is an empirical model that cannot be verified theoretically (González et al., 2010). However, Lim et al. (2019) validated the accuracy of the PBSE by comparing its static equilibrium planform with the numerical result from the calculated wave diffraction effect using the LSTR formula (USACE, 2002). Wave data were extracted from Wave Information Network of Korea (WINK) which provided incident waves observed from September 27, 2013, at 10:30 to November 21, 2016, at 9:30 on the east coast of South Korea (37° 24' 00.0" N, 129° 14' 05.2" E). These are depicted in Fig. 2, showing the time series of significant wave height, peak wave period, and significant wave direction, respectively. A total of 55,235 data points were extracted at an interval of 30 minutes, which give the average wave height, period, and direction of 0.7963 m, 7.54 sec, and 48. 72°, respectively.

https://doi.org/10.5194/nhess-2023-166
Preprint. Discussion started: 18 October 2023

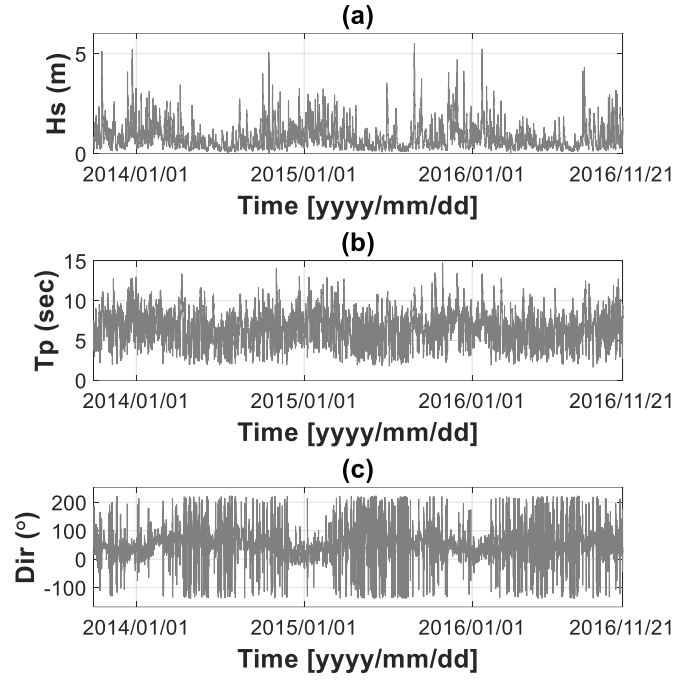

Figure 2: Temporal distribution of wave data observed on the east coast of South Korea: (a) significant wave height; (b) peak wave period; (c) significant wave direction.

Figure 3 shows joint probability distribution to analyze whether a correlation can be found in the annual mean wave heights versus the period and wave heights versus wave directions, respectively. The graphic result indicates that the most frequent wave height was less than 0.5 m, whereas the most frequent wave direction was from NE, during the period of wave observation.

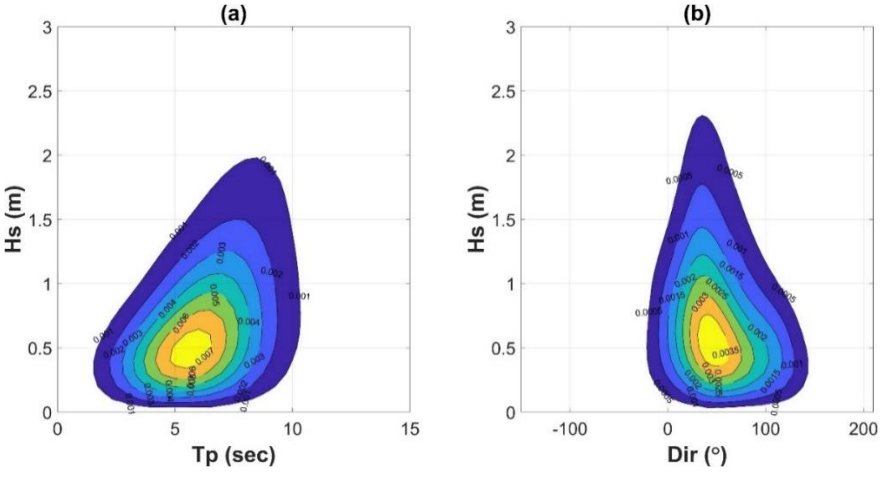

Figure 3: Joint probability distribution of annual mean wave data on the east coast of South Korea: (a) wave height versus wave period and (b) wave height versus wave direction.

https://doi.org/10.5194/nhess-2023-166
Preprint. Discussion started: 18 October 2023

Natural Hazards and Earth System Sciences
Discussions

In addition, from the distribution of annual mean wave direction and consideration of wave diffraction effect, the results are presented in Fig. 4, in which the equilibrium shoreline changes due to the construction of a gamma-shaped (Γ) breakwater that causes the deformation of breaking waves along the curved diffracted wave crests. Lim et al. (2019) compute the change in wave direction for the diffracted wave crest and apply the diffracted wave height to calculate the LSTR for the curved shape. Although only a simple wave diffraction model is used, the calculated planform is in good agreement with the result of the PBSE.

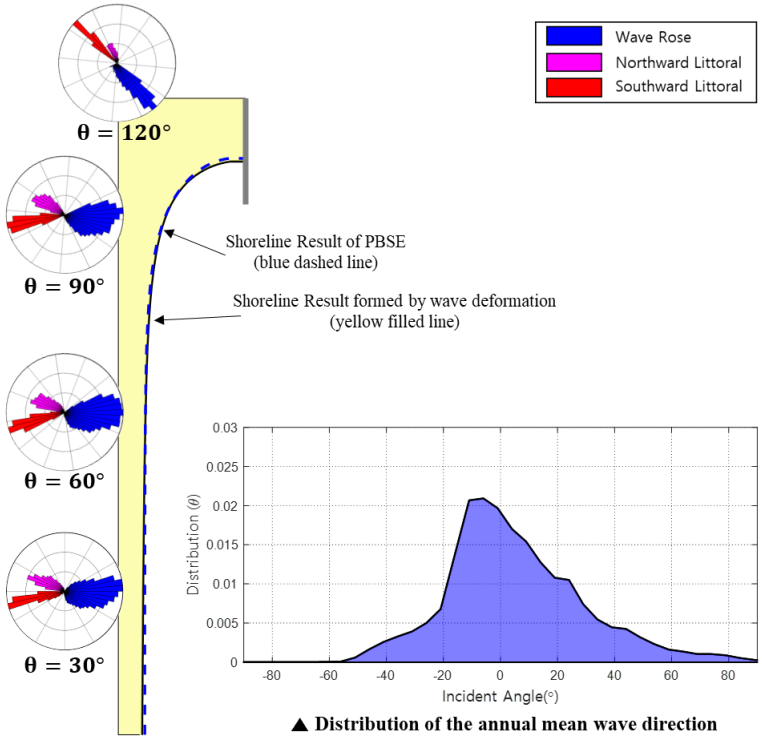

Figure 4: Comparison between the static equilibrium shoreline calculated using wave data (line filled with yellow) and the parabolic bay shape equation (blue dashed line).

3. Static equilibrium due to construction of a submerged detached breakwater

3.1 Longshore sediment transport rate

Longshore sediment transport rate (LSTR) affects shoreline changes. Although there are several different approaches used to quantify the LSTR, the empirical relationship between LSTR and energy flux established by Komar and Inman (1970) has been the most popular form (Shore Protection Manual, 1984, 2002; Kamphuis, 2002; Bayram et al., 2007; van Rijin, 2002, 2014; Lim and Lee, 2023). Among these, the CERC formula using breaking wave condition is given by,

$$Q_l = \frac{K\sqrt{g/\kappa}}{16(s-1)(1-p)} H_b^{\frac{5}{2}} \sin 2\alpha_b = C' H_b^{\frac{5}{2}} \sin 2\alpha_b \quad (2)$$

https://doi.org/10.5194/nhess-2023-166
Preprint. Discussion started: 18 October 2023

Natural Hazards and Earth System Sciences
Discussions

where Q_l is LSTR, H_b is wave height at the breaking point, and α_b is an angle between the breaking wave crest line and the shoreline. The subscript b in Eq. (2) refers to wave data at the breaking point, while parameters s, p, κ, g, and K are specific gravity of beach sand, porosity of beach sand, breaking index, acceleration of gravity, and LSTR coefficient respectively. And C' is a coefficient to represent the characteristics of sand, which has a value of approximately 0.0847. Herein, $s = 2.57$, $p = 0.35$, $\kappa = 0.78$, $g = 9.81\ \mathrm{m}/s^2$, and $K = 0.39$, which are used for most beach sands.

Because most wave data are observed/recorded in deep water rather than at breaking point, deep water wave property is preferred for direct calculation of the LSTR. Assuming depth contours to be straight and parallel to a straight shoreline, Eq. (2) can be expressed in deep water wave data (Dean and Dalrymple, 2002), such as,

$$Q_{l,O} = C'_O H_O^{2.4} T_O^{0.2} \cos \alpha_O^{1.2} \sin \alpha_O \quad (3)$$

where subscript O represents deep water wave condition. T_O is the wave period at the deep water. C'_O is taken approximately 0.0313 for most of the sand under the assumption that the wave direction in the surf zone is negligible. Also, because incident wave direction in deep water varies concerning shoreline direction, the prevailing direction of $Q_{l,O}$ must be adjusted using Eq. (4), for the condition that shoreline angle β (i.e., from N, the north) and incident wave direction θ_O, as shown in Fig. 5,

$$\alpha_O = \frac{\pi}{2} - \theta_O + \beta \quad (4)$$

Herein, a positive value for LSTR indicates the direction of transport heading southward, while a negative value for heading northward. When a shoreline aligns in a North-South direction and facing eastward, $\beta = 0°$ and waves approaching from the east. On the other hand, when a shoreline facing west, $\beta = 180°$ (clockwise from the N) (Fig. 5).

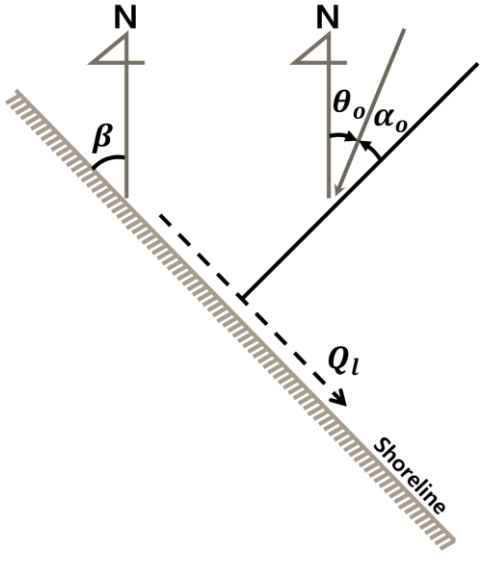

Figure 5: Direction of LSTR according to the angle of the incident wave and the shoreline from the true north (Lim et al., 2022b).

https://doi.org/10.5194/nhess-2023-166
Preprint. Discussion started: 18 October 2023

Natural Hazards and Earth System Sciences
Discussions

For example, with the wave data observed for Maengbang Beach on the central east coast of South Korea, shoreline changes can be estimated using directional distribution of LSTR (Fig. 6). When the predominant wave direction is 42.2° (the shore normal measured clockwise from North), no LSTR occurs (Fig. 6). In summer, northbound LST distributes relatively evenly, exhibiting a normal distribution, while in winter, the southbound LST. Incoming waves during winter mostly cause the development of southward LSTR, on the other hand, the sediment gets to be transported to the north when the waves flow in during summer (Lim et al., 2022b). If no long-term shoreline changes are found, it is noted that the total northward and southward LSTR balances out, yielding the net LSTR is zero (0). However, if the structure is built, incoming waves get obstructed or transmitted. To maintain the LSTR balance again, the shoreline redistributes, leading to changes in the equilibrium shoreline. Further details on how the shoreline changes behind the SDBW are provided in Section 3.3.

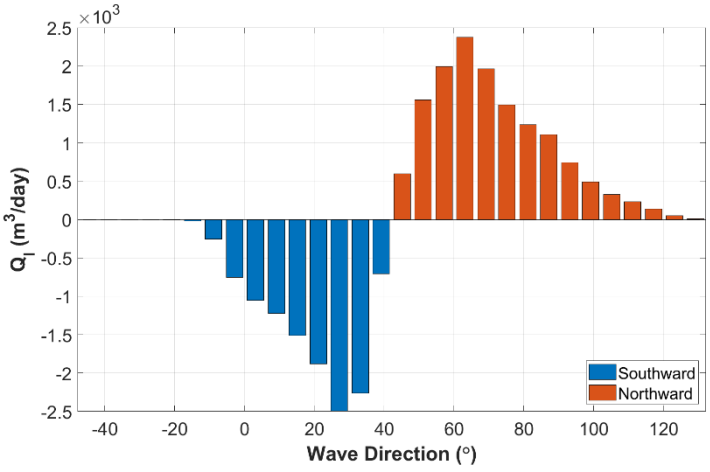

Figure 6: Directional distribution of the calculated LSTR on Maengbang Beach.

3.2 Wave transformation induced by a submerged detached breakwater

3.2.1 Wave diffraction behind an EDBW

Let us consider wave diffraction, when incident waves approach normally from deepwater to a moderate EDBW parallel to a straight shoreline. Varying water depths behind the structure allow wave refraction and diffraction until reaching an equilibrium state shoreline without reflection. However, it is difficult to estimate wave diffraction caused by the port structure or topography. Therefore, in this study, wave diffraction is applied to LSTR assuming simple equations. Based on a set of simple equations below (Eq. 5a –5c) for diffraction coefficient K_d, Lim et al. (2019) estimated the effect of a gamma-shaped (Γ) EDBW on LSTR (see Fig. 4).

$$K_d(\zeta_i) = 0 \qquad \text{for } \zeta_i - \theta < -\frac{\pi}{8} \tag{5a}$$

$$K_d(\zeta_i) = cos^2\left[2\left(\zeta_i - \theta - \frac{\pi}{8}\right)\right] \qquad \text{for } -\frac{\pi}{8} \le \zeta_i - \theta \le \frac{\pi}{8} \tag{5b}$$

https://doi.org/10.5194/nhess-2023-166
Preprint. Discussion started: 18 October 2023

Natural Hazards and Earth System Sciences
Discussions

$$K_d(\zeta_i) = 1 \qquad \text{for} \quad \zeta_i - \theta > \frac{\pi}{8} \tag{5c}$$

where ζ_i is a function of incident wave direction (θ) measured radially clockwise from incident wave crest line at one end (the focus) of the EDBW (Fig. 1). Equation (5) indicates wave diffraction coefficients (K_d) decreases as θ increases toward the shallow zone behind the EDBW, which corresponds to the wave direction in the wave rose diagram. K_d = 0.5 is taken when $\theta - \zeta_i$ is at 90° (Fig. 7). This figure also shows the effects of diffraction through the focus point angle θ at 0°, 30°, 90°, 120°, 150° and 180° respectively.

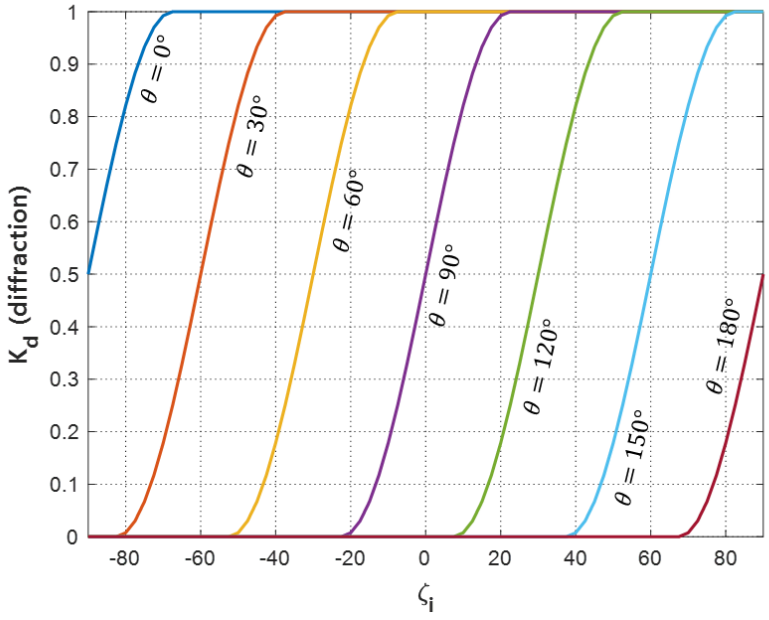

Figure 7: Effects of wave diffraction depending on incident wave direction ($\theta = 0°, 30°, 90°, 120°, 150°, 180°$).

3.2.2 Wave transmission

Unlike an EDBW that obstructs incoming waves, wave transmission occurs since an SDBW transmits and partially reflects incident wave energy. As shown in Fig. 8, the initial incident waves may reflect and transmit through the structure. Applying the principle of energy conservation, incident wave energy (E_i) equals the sum of three types of wave energy,

$$E_t + E_r + E_{dis} = E_i \tag{6}$$

where E_r, E_t, E_{dis} and E_i represent wave energy due to reflection, transmission dissipation, and incident waves, respectively.

https://doi.org/10.5194/nhess-2023-166
Preprint. Discussion started: 18 October 2023

Natural Hazards and Earth System Sciences
Discussions

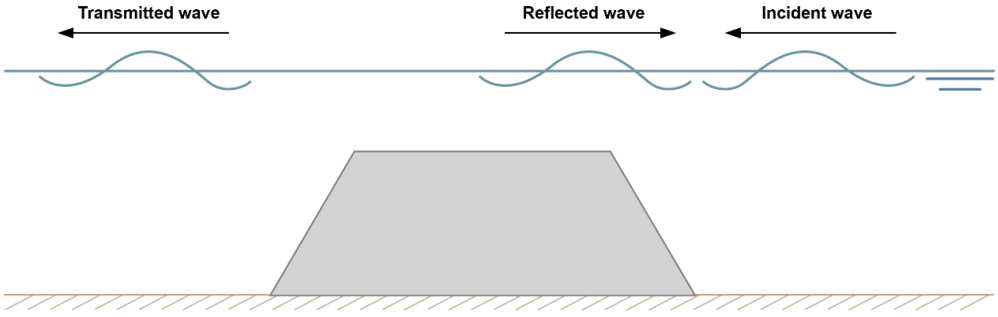

Figure 8: Definition sketch of reflection and transmission of waves induced by an SDBW.

From Eq. (6), the dimensionless rate of wave energy for transmission, reflection, and dissipation satisfy the relationship,

$$K_t^2 + K_r^2 + K_{dis}^2 = 1 \quad (7)$$

where K_t and K_r denote dimensionless transmission rate and reflection rate, respectively, for each wave height ratio concerning the incident wave height (Eqs. 8a–8b), If energy loss is ignored, then transmission coefficient behind the structure will be reflected.

$$K_t = \frac{H_t}{H_i} \quad (8a)$$

$$K_r = \frac{H_r}{H_i} \quad (8b)$$

Laboratory experiments have been conducted to derive the formula for the transmission coefficient over transmissible structures (Takayama et al., 1985; d'Angremond et al., 1996; Lee et al., 2020). Jeong et al. (2021) also observed the transmission coefficient for SDBWs in field conditions and derived a formula employing an error function (Section 4.1).

3.3 Prediction of Static Equilibrium behind Submerged Detached Breakwater

As described in Section 3.1, it is assumed that the shoreline is in equilibrium when the annual average LSTR is zero (0). However, for net LSTR not equal to zero, shoreline change would occur at downdrift or behind SDBW or EDBW, due to wave diffraction and transmission. With the equilibrium shoreline rotating along the curved planform, the value of LSTR can be calculated from wave data for specific locations on the shoreline. The result shown in Fig. 9 illustrates the wave rose diagram and the littoral drift diagram, which present the effect of SDBW that causes shoreline rotation.

https://doi.org/10.5194/nhess-2023-166
Preprint. Discussion started: 18 October 2023

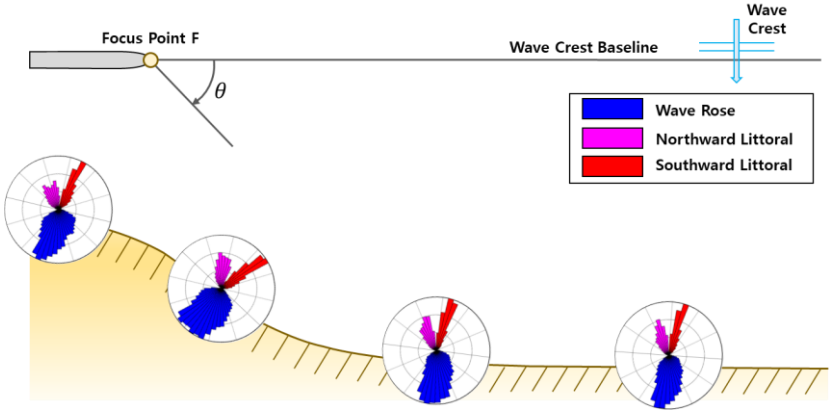

Figure 9: Wave and littoral drift roses behind an SDBW calculated from wave data.

To show the shoreline rotation angles at Maengbang Beach (Sec. 2.1), where LSTR is balanced using the CERC formula, the impacts of SDBW on wave deformation can be assessed from wave information (Fig. 9). In Fig. 10, the red dashed line represents shoreline change resulting from a coastal structure, such as an EDBWs, while the blue lines show shoreline rotation angle as a function of transmission coefficient over an SDBW ranging from 0.1 0.9 at an interval of 0.1, depending on the wave setup and tidal conditions.

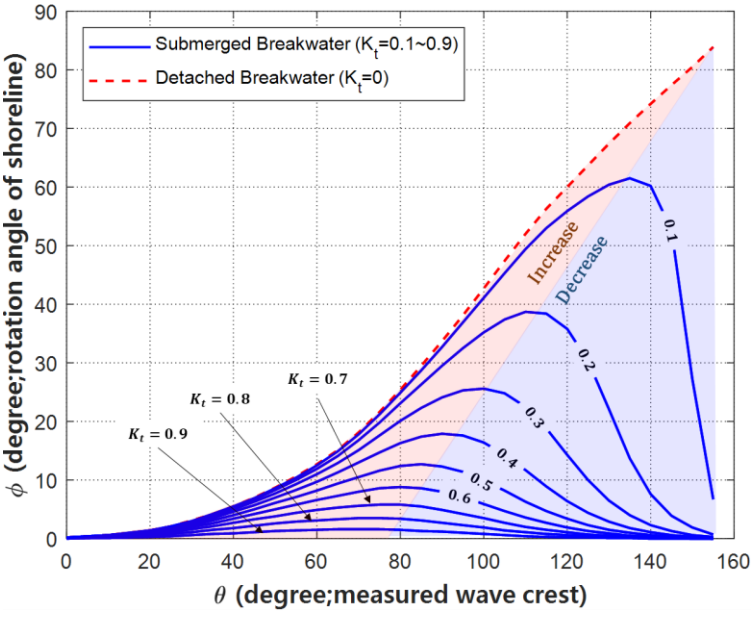

Figure 10: Shoreline rotation angle showing the effect of transmission coefficient behind an SDBW.

The rotation angle of the SEP behind the SDBW can be estimated using the methodology. Therefore, it is necessary to convert the rotation angle to the shoreline. Shoreline rotation angles (θ_n) can be calculated from a function of the radial distance R, measured from the focus (Fig. 1) as follows,

https://doi.org/10.5194/nhess-2023-166
Preprint. Discussion started: 18 October 2023

Natural Hazards and Earth System Sciences
Discussions

$$R_{n+1} = R_n \frac{sin(\theta_n - \varphi)}{sin(\theta_{n+1} - \varphi)} \quad \text{for } \theta_n \geq \beta \tag{9a}$$

$$R_n = \frac{a}{sin\,\theta_n} \quad \text{for } \theta_n < \beta \tag{9b}$$

where φ is the shoreline rotation angle. The static equilibrium shoreline affected by an SDBW can be predicted by applying Eqs. (9a)-(9b). Thus, prediction of the SEP can be achieved with only the focus point (i.e., diffraction reference point) and the downdrift control point. As proposed by Lim et al. (2022a), the predicted SEP caused by an SDBW can be achieved by using polar coordinates. Figure 11 shows the SEP behind an SDBW (100 m in length and at 50 m offshore) with transmission coefficients of 0.2, 0.4, 0.6, and 0.8, respectively.

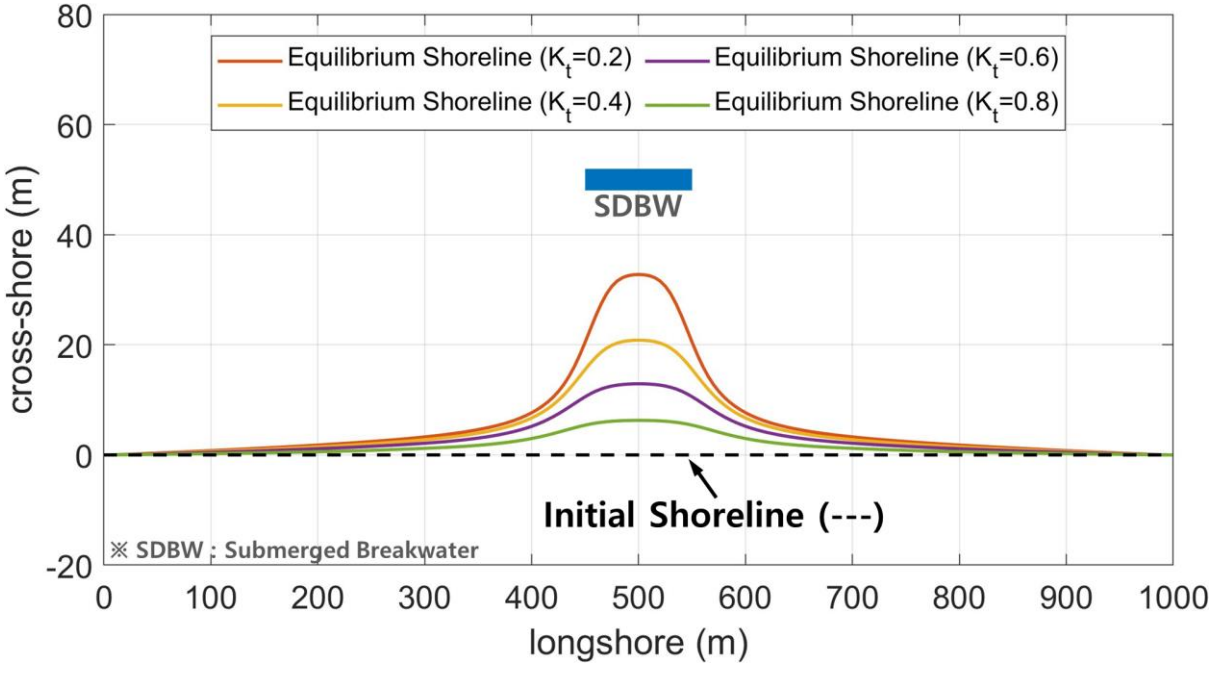

Figure 11: Static equilibrium shoreline behind an SDBW with various transmission coefficients ($K_t = 0.2, 0.4, 0.6$ and 0.8).

4. Application of shoreline change model

4.1 Study site

The methodology presented in this study is applied to predict shoreline changes due to the construction of SDBWs at Bongpo-Cheonjin (38°15'N, 128°33'E; Fig. 12) on the east coast of South Korea and the results are compared with that from field observation. The beach is approximately 1.1 km long, with a crenulated-shaped bay between two harbors; Cheonjin Harbor in the northern and Bongpo Harbor to the southern, respectively. Lim et al. (2021b) quantitatively evaluated the erosion risk caused by different factors, such as background erosion, redistribution erosion, and episodic erosion. Among them, and more specifically, the stage-wise extension of the Cheonjin Harbor breakwater has caused unrecoverable damages to the south part

https://doi.org/10.5194/nhess-2023-166
Preprint. Discussion started: 18 October 2023

Natural Hazards and Earth System Sciences
Discussions

of the beach. This prompted the Ministry of Oceans and Fisheries in Korea to start an improvement project in which four SDBWs (490 m in total) and one groin (GR) 40 m long were constructed (Fig. 12) to mitigate erosion. The construction project commenced in 2017 and completed in November 2019.

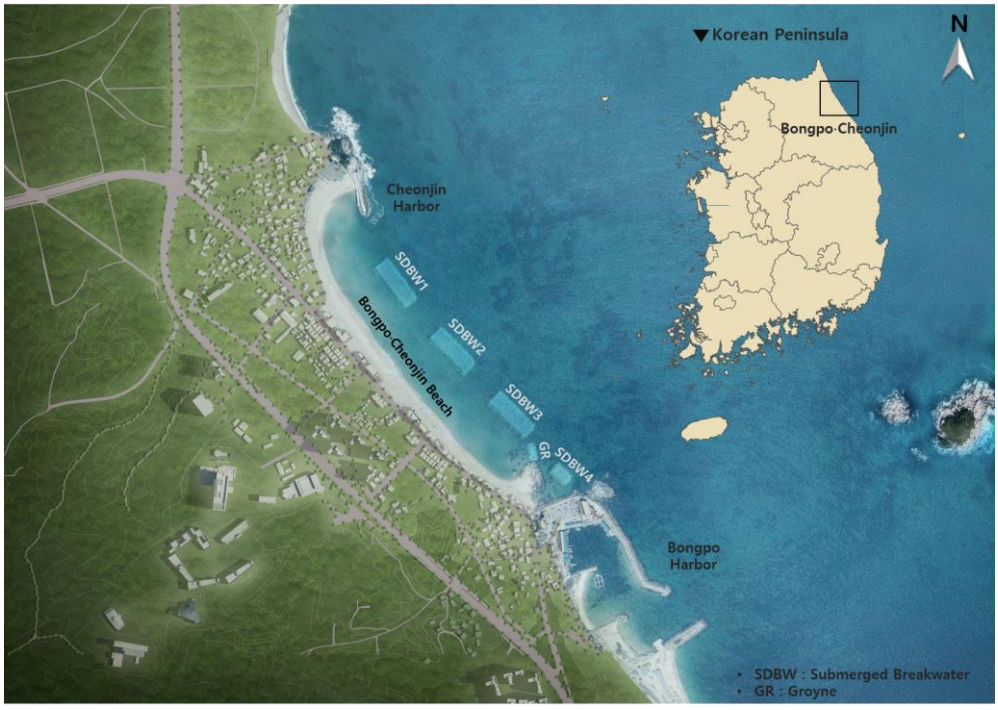

Figure 12: Location of Bongpo-Cheonjin Beach and coastal structures to mitigate beach erosion.

Jeong et al. (2021) observed the waves in front of and behind the SDBWs at Bongpo-Cheonjin during the passage of typhoon Krosa over the Korean peninsula in 2019. Using the observed wave data, they proposed a formula with an error function to estimate the transmitted wave height over an SDBW,

$$H_t = \kappa R_c erf\left(\frac{H_i}{R_c}\right) \quad (10)$$

where R_c is the effective crest height of aanSDBW. For Bongp-Cheonjin Beach, R_c is approximately 1.25 m (Jeong et al., 2021). Therefore, transmission coefficient K_t becomes:

$$K_t = \kappa R_c erf\left(\frac{H_i}{R_c}\right)/H_i \quad (11)$$

Figure 13(a) compares the observed wave heights in front of and behind the SDBWs at Bongpo-Cheonjin with the error function of Eq. (10), while Fig. 13(b) shows the observed transmission coefficient compared to the results of error function of Eq. (11). As the average incident wave height in Bongpo-Cheonjin was 0.76 m, therefore, the calculated transmission coefficient is approximately 0.8 using Eq. (11), as shown in Fig. 13(b) (Jeong et al., 2021).

https://doi.org/10.5194/nhess-2023-166
Preprint. Discussion started: 18 October 2023

Natural Hazards and Earth System Sciences
Discussions

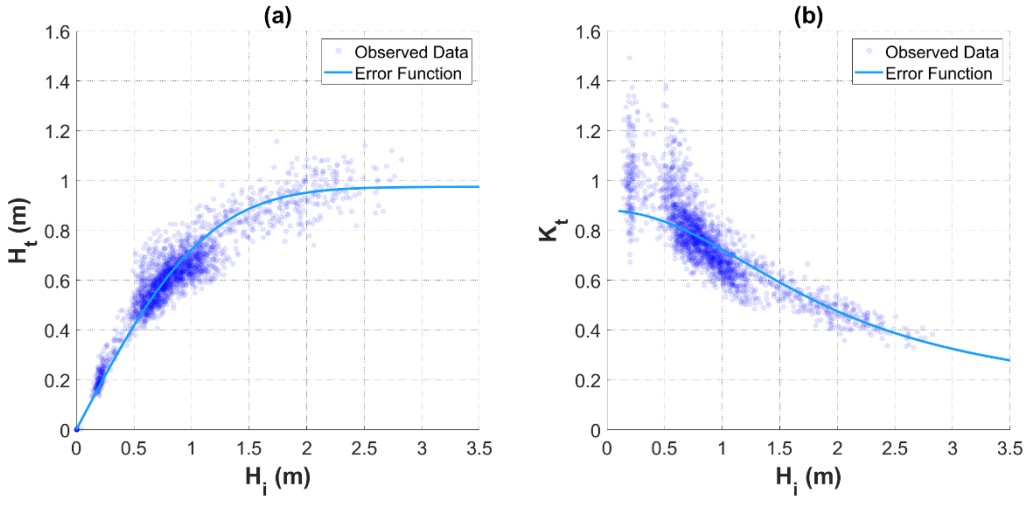

Figure 13: Analysis of transmission coefficient for SDBW on Bongpo·Cheonjin Beach: (a) incident wave height-transmitted wave height; (b) incident wave height–transmission coefficient.

4.2 Verification of the predicted shoreline

In South Korea, coastal video monitoring program using CCTV has been progressively established for coastal management since 2003 (Lim et al., 2022b). So far approximately 91.8 % of the area of Bongpo-Cheonjin Beach has been covered by four CCTVs from May 2015 to the present (Fig. 14), in which the coordinates on the video reference points have been set for extracting the shoreline information from CCTV images. A geometric transformation formula of Lippmann and Holman (1989) can be applied to transform from video to ground coordinates.

Figure 14: Video monitoring using four CCTVs at Bongpo-Cheonjin Beach (MOF, 2019; © National Geographic Information Institute (NGII), Korea).

From beach images, salient shapes during relatively high waves are extracted to verify the methodology presented in this paper. This is carried out by applying the wave data provided by the Korea Meteorological Administration, for high waves occurring

https://doi.org/10.5194/nhess-2023-166
Preprint. Discussion started: 18 October 2023

Natural Hazards and Earth System Sciences
Discussions

on Bongpo-Cheonjin Beach from December 18, 2020, to January 7, 2021. Under the assumption that the depth contours tend to be straight and parallel to the shoreline, the time series shows changes in calculated breaking wave height and peak wave period using the data observed in the deep sea. The results reveal the mean wave height, period and direction are 1.09 m, 7.42 sec, and 50.8°, respectively.

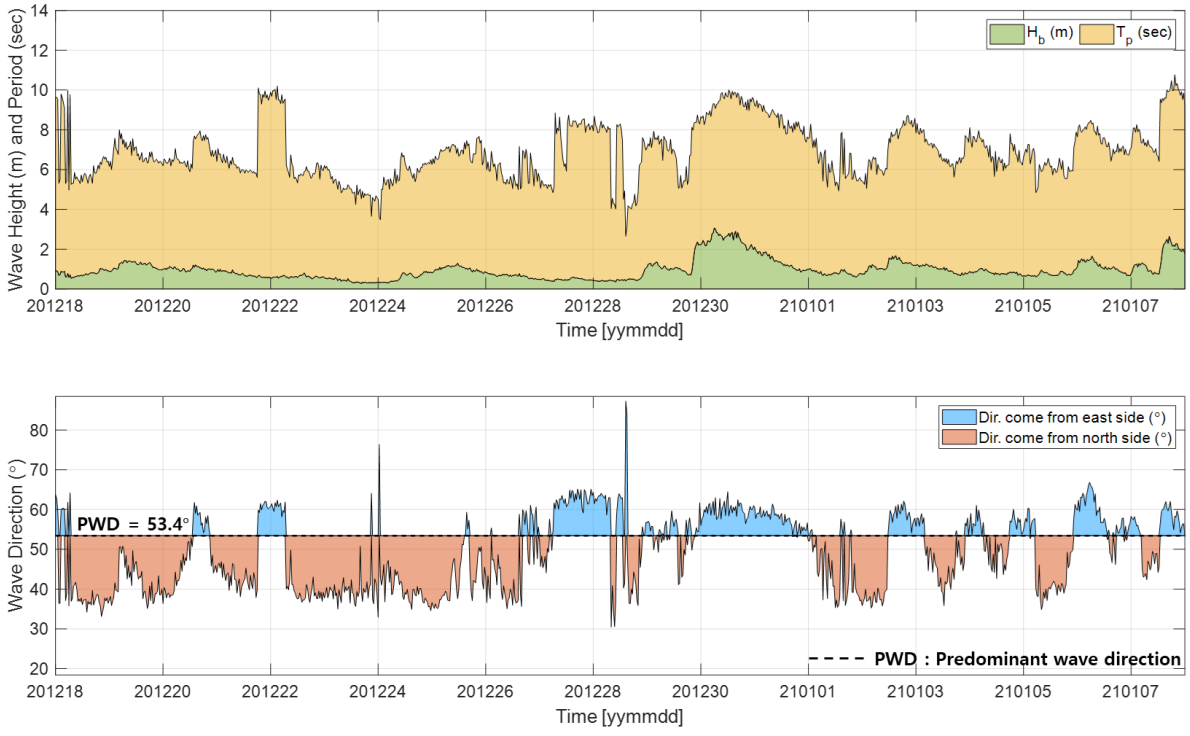

Figure 15: Temporal series of breaking waves at Bongpo·Cheonjin Beach from December 18, 2020, to January 7, 2021.

Lim et al. (2022a) transformed the Cartesian coordinate system into polar coordinates for predicting the SEP shoreline change at Bongp-Cheonjin. The predominant wave direction is N53.4°E from the circle fitting of Bongpo-Cheonjin Beach using MeePaSoL software (Lee, 2015; Lim et al., 2022a). Figure 16 compares the shoreline planform extracted from CCTV images with that predicted using the approach presented in this study, assuming a transmission coefficient of 0.49 from a breaking index of 0.55 (using significant wave height). It also shows the calculated SEP planform is in good agreement with the observed, and the deposition width of the salient, is also similar to the observed.

https://doi.org/10.5194/nhess-2023-166
Preprint. Discussion started: 18 October 2023

Natural Hazards and Earth System Sciences
Discussions

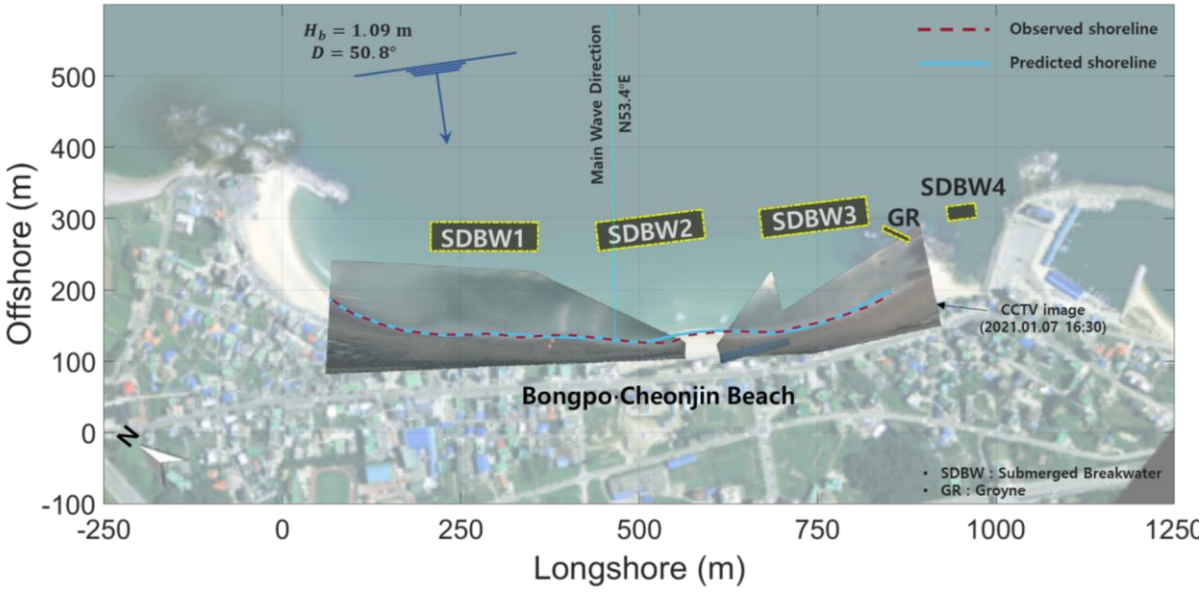

Figure 16: Comparison of shoreline extracted from CCTV image and that predicted by the methodology in this study (© NGII, Korea).

4.3 Estimation of equilibrium shoreline

SEP behind the SDBWs at Bongpo-Cheonjin is calculated using transmission coefficient K_t = 0.8 over the submerged structures. In Fig. 17, the solid line represents the predicted SEP under waves and the aerial photograph is the shoreline before the construction of the SDBWs and groin. Upon comparing the calculated results with the shoreline on the existing aerial photograph, no noticeable shoreline changes have occurred in the north part of the beach, while minor deposition is behind SDBW1 which was constructed last. Small salient SDBW2 was constructed in the center of the beach, salient was formed at the sagged point of the shoreline behind the structure, which is located on the southern side from the center. Lastly, because SDBW3 and the groin were built closely to each other, they work collectively as a long groin, resulting in shoreline advancement in the south part of the beach. Overall, it may be concluded that the structures constructed at Bongpo-Cheonjin have achieved the purpose of mitigating the potential beach.

https://doi.org/10.5194/nhess-2023-166
Preprint. Discussion started: 18 October 2023

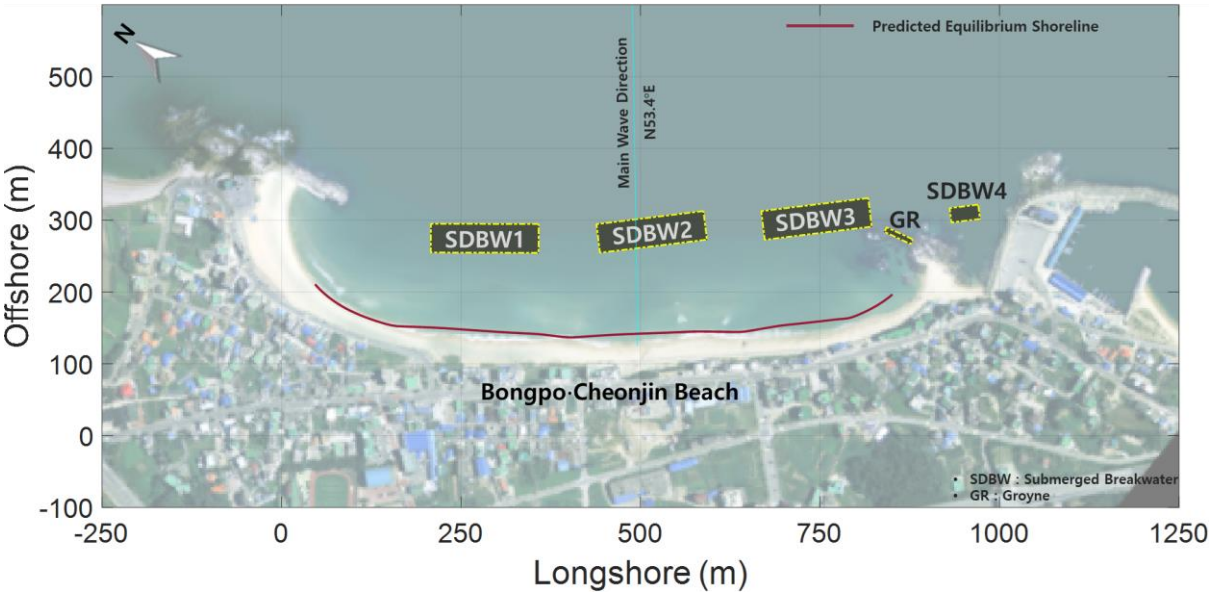

290 **Figure 17: Estimation of SEP due to construction of SDBWs and a groin on Bongpo-Cheonjin Beach ($K_t = 0.8$; © NGII, Korea).**

4.4 Estimation of shoreline change due to storm waves

Assume storm waves acting on Bongpo-Cheonjin, shoreline retreat behind the four SDBWs can be predicted using the methodology presented in this paper. Lim et al. (2021b) analyzed the observed shoreline data and reported the eroded shoreline with a 30-year return period was approximately 19.75 m. The eroded shorelines were estimated by setting control points from
295 the location in which about 19.75 m was moved backward from the initial ones. This occurred on a narrow stretch between SDBW1 and SDBW2 as indicated in Fig. 18.

https://doi.org/10.5194/nhess-2023-166
Preprint. Discussion started: 18 October 2023

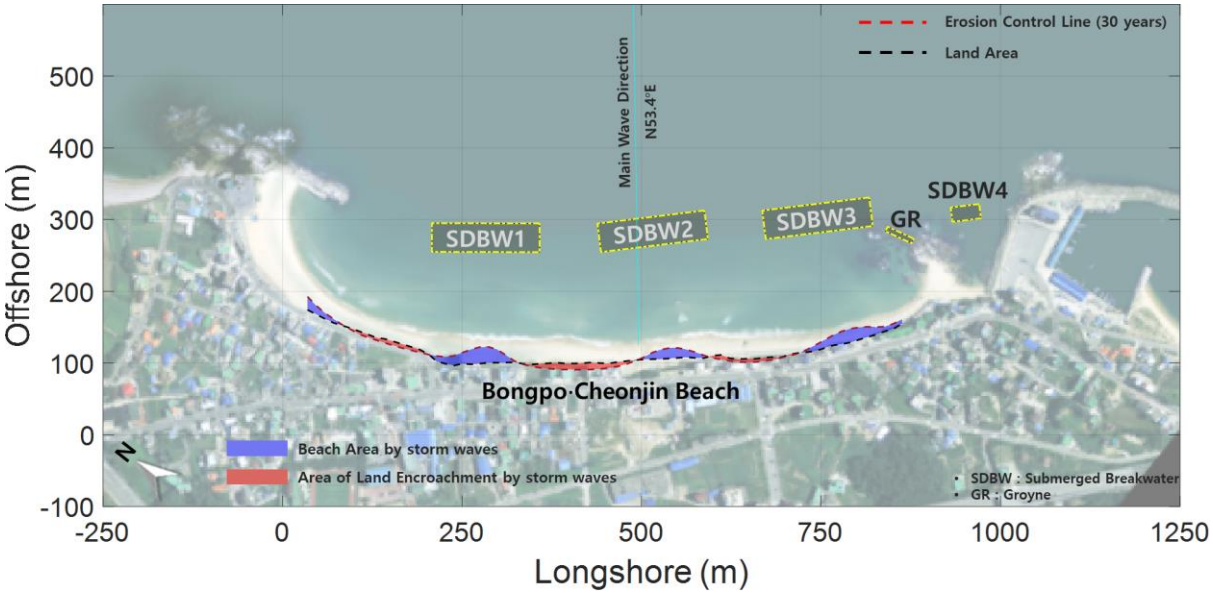

Figure 18: Shoreline retreat due to storm waves with 30-year return period (© NGII, Korea).

5. Discussions

Limitations of the methodology presented in this study are discussed, as well as its practical applicability for coastal engineering design and management.

(1) Difficulties exist in the accurate prediction of wave deformation caused by the presence of submerged transmissible coastal structures, such as submerged DBWs (SDBWs) consisting of precast concrete blocks. Thus, the SEP in the vicinity of these structures should be considered as an estimate using the relatively simple equation for wave diffraction and transmission.

(2) In this paper, long-term wave observation data in the East Sea of South Korea are used to estimate shoreline changes behind SDBWs at Bongpo-Cheonjin. To enhance the confidence of the estimation, it is necessary to apply the methodology to other beaches with different wave-hydrodynamic settings and nearshore bathymetry. Although the methodology to estimate the effect of an SDBW on the SEP behind is shown, the influence of the gap (spacing) in a multi-SDBW system is not assessed, Thus, further research is required to improve the accuracy of estimation.

(3) A one-line shoreline change model incorporating shoreline rotation in the wave diffraction zone is used to simulate behind an SDBW with a specific transmission coefficient. The governing equation was originally proposed by Pelnard-Considère (1956) for a system of short groins without wave diffraction to determine shoreline positions based on LSTR differences. The model assumes erosion and deposition within an active volume measured from the berm to the depth of closure is constant (Eq. 12).

https://doi.org/10.5194/nhess-2023-166
Preprint. Discussion started: 18 October 2023

Natural Hazards and Earth System Sciences
Discussions

$$\frac{\partial x}{\partial t} + \frac{1}{(h_c+h_B)}\frac{\partial Q_l}{\partial y} = 0 \quad (12)$$

where h_c is the depth of closure and h_B is the berm height. the value of each LSTR Q_l can be estimated using the CERC formula (USACE, 1984). Shoreline position is represented by Cartesian coordinate in which x is measured in the cross-shore direction, while yy is in the alongshore direction.

The value of Q_l can be calculate by deep water wave data, as in Eq. (3), but with modified wave angle α_m along the rotated SEP calculated by the PBSE, instead of α_0,

$$Q_{l,O} = C'_O H_O^{2.4} T_O^{0.2} \cos \alpha_m^{1.2} \sin \alpha_m \quad (13)$$

where α_m refers to an angle of diffracted waves within the shadow zone of a SDBW (Lim et al., 2021a) and wave transmission coefficient per Fig. 10.

Finally, the results of the numerical calculation are depicted in Fig. 19 for shoreline changes after the construction of SDBWs on Bongpo-Cheonjin Beach, shoreline changes for 1 month, 3 months, and 1 year, respectively, assuming active vertical depth 7.0 m with wave transmission coefficient for normal waves as-0.8.

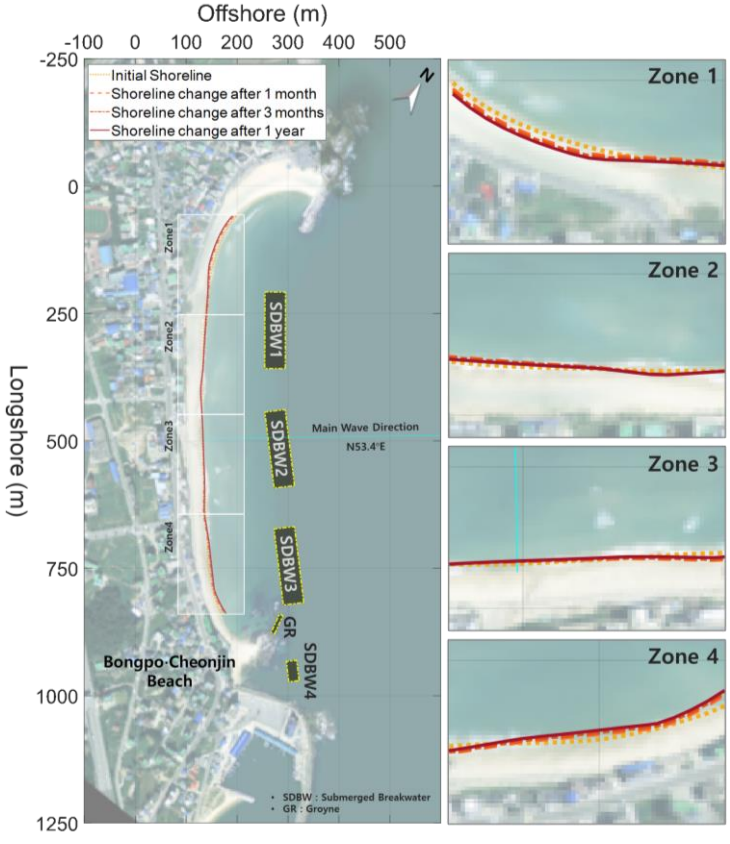

Figure 19: Simulation of shoreline change model due to the construction of SDBWs and a GR in Bongpo-Cheonjin Beach (© NGII, Korea).

https://doi.org/10.5194/nhess-2023-166
Preprint. Discussion started: 18 October 2023


Natural Hazards and Earth System Sciences Discussions

6. Conclusion

This study presents a methodology to estimate the shoreline change behind multiple SDBWs constructed on an embayed beach on the east coast of South Korea. Applying the observed deepwater wave data, Jeong et al. (2021) determined the wave transmission coefficient (K_t about 0.8) for the SDBWs at Bongpo-Cheonjin and also established the error function between incident waves and transmitted waves. The effect of wave diffraction and transmission through the submerged structures are considered, as well as the variation of the calculated LSTR with its magnitude varies (rotates) along the curved equilibrium shoreline.

Unlike the EDBWs, the shore-normal direction on the stretch of beach behind the SDBWs at Bongpo-Cheonjin tends to increase and then decrease, due to the effect of wave transmission and diffraction. The computed wave angles, as a function of the radial distance R and angle θ around the updraft control point (the focus) in Fig. 1, are then used to calculate the change in the LSTR and equilibrium shoreline.

Accurate prediction of shoreline changes behind SDBWs is important for mitigating beach erosion, because a small salient may form behind a SDBW which is accompanied by erosion in the gap section between adjacent SDBWs. Therefore, the results derived from this study, on predicting how a shoreline may change after installing a series of SDBWs, will benefit the technical designers and coastal managers.

Data availability

Data sets used in this work can be requested by email from the author.

Author contributions

Supervision, J.-L.L.; Writing—original draft, C.L.; Writing—review & editing, C.L., J.K. and J.L.-L.; Analysis, C.L., J.K. and J.L.-L.; Data acquisition, C.L., and J.-B.K. All authors have read and agreed to the published version of the manuscript.

Competing interests

The authors declare no conflicts of interest.

Acknowledgments

This research was supported by the Korea Institute of Marine Science & Technology Promotion (KIMST), funded by the Ministry of Oceans and Fisheries, Korea (RS-2023-00256687).

https://doi.org/10.5194/nhess-2023-166
Preprint. Discussion started: 18 October 2023


Natural Hazards and Earth System Sciences Discussions

References

Ab Razak, M. S., Jamaluddin, N. and Mohd Nor, N. A. Z.: The planform stability of embayed beaches on the west coast of Peninsular Malaysia, J. Technological Science & Engineering, 80, 4, 33–42, 2018a.

Ab Razak, M. S, Mohd Nor, N. A. Z. and Jamaluddin, N.: Planform stability of embayed beaches on the east coast of Peninsular Malaysia, Journal of Engineering Science and Technology, Taylor's University, 13, 2, 435–448, 2018b.

Ahrens, J. P. and Cox, J.: Design and performance of reef breakwaters, J. Coastal Res., 1, 61–75, 1990.

Anh, D. T. K., Stive, M. J. F., Brouwer, R. L. and de Vries, S.: Analysis of embayed beach planform stability in Danang, Vietnam. E- Proc. 36th IAHR World Congress, The Hague, The Netherlands, 6, 2015.

Bayram, A., Larson, M. and Hanson, H.: A new formula for the total longshore sediment transport rate, Coastal Eng., 54, 700–710, 2007.

Bowman, D., Guillén, J., López, L. and Pellegrino, V.: Planview geometry and morphological characteristics of pocket beaches on the Catalan coast (Spain), Geomorphology, 108, 3, 191–199, 2009.

CERC: Shore Protection Manual, 4th Ed. U.S. Army Corps of Engineers, Waterways Experiment Station, Coastal Engineering Research Center, U.S. Government Printing Office, Washington, D.C., 1984.

d'Angremond, K., Van der Meer, J. W. and De Jong, R. J.: Wave transmission at low-crested structures, Proc. 25th Inter. Conf. on Coastal Engineering, ASCE, 3305–3318, https://doi.org/10.1061/9780784402429.187, 1996.

Dally, W. R. and Pope, J.: Detached breakwaters for shore protection, Technical Report CERC-86-1, U.S. Army Engineer Waterways Experiment Station, Vicksburg, MS, 1986.

Dean, R. and Dalrymple, R.: Coastal Processes with Engineering Applications, Cambridge: Cambridge University Press, Cambridge, UK, 475 pp, https://doi.org/10.1017/CBO9780511754500, 2002.

González, M., Medina, R. and Losada, M. A.: On the design of beach nourishment projects using static equilibrium concepts: Application to Spanish coast, Coastal Engineering, 57, 2, 227–240, 2010.

Gourlay, M. R.: Beach processes in the vicinity of offshore breakwaters, Proc. Fifth Australian Conference on Coastal and Ocean Engineering, 129–134, 1981.

Hanson, H. and Kraus, N. C.: Genesis: Generalized Model for Simulating Shoreline Change, Report 1: Reference Manual and Users Guide. U.S. Army Corps of Engineers, Coastal Engineering Research Center, Technical Report CERC-89-19, 1989.

Herbich, J. B.: Shoreline change due to offshore breakwaters, Proc. 23rd Cong. Ass. Hyd. Engrs., 317–327, 1989.

Herrington, S. P., Li, B. and Brooks, S.: Static equilibrium bays in coast protection, Marine Engineering Group, Institution of Civil Engineers, Thomas Telford, London, Online May 25, 2015. https://doi.org/10.1680/maen.2007.160.2.47, 2007.

Hsu, J. R. C. and Evans, C.: Parabolic bay shapes and applications, Proc. Inst. Civil Engineers, Part 2, 87, 557 –570, 1989.

Hsu, J. R., C. and Silvester, R.: Accretion behind single offshore breakwater, J. Waterway, Port, Coast. Ocean Eng., ASCE, 116, 3, 362–381, 1990.

https://doi.org/10.5194/nhess-2023-166
Preprint. Discussion started: 18 October 2023

Hur, D. S.: Deformation of multi-directional random waves passing over an impermeable submerged breakwater installed on a sloping bed. Ocean Engineering, 31, 1295–1311, 2004.

Inman, D. L. and Frautschy, J. D.: Littoral processes and the development of shoreline, Proc. Santa Barbara Specialty Conf. Costal Eng., ASCE, 511–535, 1965.

Joeng, J. -H., Kim, J. H. and Lee, J. -L.: Analysis of wave transmission characteristics on the TTP submerged breakwater using a parabolic-type linear wave deformation model, Journal of Ocean Engineering and Technology, 35, 1, 82–90, 2021.

Kamphuis, J. W.: Alongshore transport of sand, Proc. 28th Int. Conf. Coastal Eng., ASCE, 2478–2490, 2002.

Kang, Y. K., Park, H. B. and Yoon, H. S.: Shoreline changes caused by the construction of coastal erosion control structure at the Youngrang Coast in Sokcho, East Korea, Journal of the Korean Society for Marine Environmental Engineering, 13, 4, 296–304, 2010.

Kim, T. -K. and Lee, J. -L.: Analysis of shoreline response due to wave energy incidence using equilibrium beach profile concept, J. Ocean Engineering and Technology, 32, https://doi.org/10.26748/ksoe.2018.4.32.2.116, 2018.

Kim, T. K., Lim, C. and Lee, J. L.: Vulnerability analysis of episodic beach erosion by applying storm wave scenarios to a shoreline response model, Frontiers Mar. Sci., 8:759067, 2021.

Kobayashi, N. and Wurjanto, A.: Wave overtopping on coastal structures, Journal of Waterway, Port, Coastal, and Ocean Engineering, ASCE, 115, 235–251, 1989.

Komar, P. D. and Inman D. L.: Longshore and transport on beaches, J. Geophys. Res., 75, 30, 5914–5927, 1970.

Lausman, R., Klein, A. H. F. and Stive, M. J. F.: Uncertainty in the application of parabolic bay shape equation: Part 1, Coastal Engineering, 57, 2, 132–141, 2010a.

Lausman, R., Klein, A. H. F. and Stive, M. J. F.: An uncertainty in the application of parabolic bay shape equation: Part 2, Coastal Engineering, 57, 2, 142–151, 2010b.

Lee, J. L.: MeePaSoL: MATLAB-GUI based software package. Sungkyunkwan University, SKKU Copyright No. C-2015-02461, 2015.

Lee, W. D., Her, D. S., Park, J. B. and An, S. W.: A study on effect of beachface gradient on 3-D currents around the open inlet of submerged breakwaters, Journal of Ocean Engineering and Technology, 23, 1, 7–15, 2009.

Lim, C., Lee, J. -L. and Kim, I. H.: Performance test of parabolic equilibrium shoreline formula by using wave data observed in East Sea of Korea, J. Coastal Res., 91, 101–105, 2019.

Lim, C., Lee, J. and Lee, J. -L.: Simulation of bay-shaped shorelines after the construction of large-scale structures by using a parabolic bay shape equation, J. Mar. Sci. Eng., 9, 43, 2021a.

Lim, C., Kim, T. K., Lee, S., Yeon, Y. J. and Lee, J. L.: Assessment of potential beach erosion risk and impact of coastal zone development: a case study on Bongpo–Cheonjin Beach, Nat. Hazards Earth Syst. Sci., 21, 3827–3842, https://doi.org/10.5194/nhess-21-3827-2021, 2021b.

Lim, C., Hsu, J. R. C. and Lee, J. L.: MeePaSoL: A MATLAB-based GUI software tool for shoreline management. Computers & Geosciences, 161, 105059, 10.1016/j.cageo.2022.105059, 2022a.

https://doi.org/10.5194/nhess-2023-166
Preprint. Discussion started: 18 October 2023

Lim, C., Hwang, S. and Lee, J. L.: An analytical model for beach erosion downdrift of groins: case study of Jeongdongjin Beach, Korea. Earth Surface Dynamics, 10, 151-163, doi:10.5194/esurf-10-151-2022, 2022b.

Lim, C., Kim, T. K. and Lee, J. L.: Evolution model of shoreline position on sandy, wave-dominated beaches, Geomorphology, 415, 15, 108409, 2022c.

Lim, C. and Lee, J. L.: Derivation of governing equation for short-term shoreline response due to episodic storm wave incidence: comparative verification in terms of longshore sediment transport, Frontier Mar. Sci., https://doi.org/10.3389/fmars.2023.1179598, 2023.

McCormick, M. E.: Equilibrium shoreline response to breakwaters, J. Waterway Port Coastal Ocean Engrg, 119, 6, 657–670, 1993.

Newman, J. N.: Propagation of water wave over an infinite step, J. Fluid Mech, 23, 399–415, 1965.

Nir, Y.: Offshore artificial structures and their influence on the Israel and Sinai Mediterranean beach, Proc. 18th Int. Conf. Coastal Engineering, ASCE, 1837–1856, 1982.

Noble, R. M.: Coastal structures' effects on shoreline, Proc. 17th Inte. Conf. Coastal Engineering, ASCE, 2069–2085, 1978.

Silveira, L. F., Klein, A. H. F. and Tessler, M. G.: Headland-bay beach planform stability of Santa Catarina State and the northern coast of São Paulo State, Brazilian Journal of Oceanography, 58, 2, 101–122, 2010.

Suh, K. and Dalrymple, R. A.: Offshore breakwaters in laboratory and field J, Waterway, Port, Coastal, and Ocean Engineering, ASCE, 113, 2, 105–121, 1987.

Tan, S. K. and Chiew, Y. M.: Analysis of bayed beaches I Static equilibrium, J. Waterway, Port, Coastal and Ocean Eng., ASCE, 120, 2, 145-153, 1993.

Takayama, T., Nagai, K. and Sekiguchi, T.: Irregular wave experiments on wave dissipation function of submerged breakwater with wide crown, Proc. 32nd Japanese Conf. Coastal Engineering, JSCE 32, 545–549, 1985.

Thomas, T., Williams, A. T., Rangel-Buitrago, N., Phillips, M. and Anfuso, G.: Assessing embayment equilibrium state, beach rotation and environmental forcing influences: Tenby Southern Wales, UK. J. Marine Science & Engineering 4, 30, 2016.

USACE: Coastal Engineering Manual (online), U.S. Army Corps of Engineers, Washington, DC. http://chl.erdc.usace.army.mil/chl.aspx?p_s&a_articles;104, 2002.

van der Meer, J. W. and Deamen, I. F. R.: Stability and wave transmission at low crested rubble mound structures, J. Waterway, Port Coastal and Ocean Engineering, ASCE, 1, 1–19, 1994.

van Rijn, L. C.: Longshore transport, Proc. 28th Int. Conf. Coastal Eng., ASCE, Cardiff, 2439–2451, 2002.

van Rijn, L. C.: A simple general expression for longshore transport of sand, gravel and shingle, Coastal Eng., 90, 23–39, 2014.

Wamsley, T., Hanson, H. and Kraus, N. C.: Wave transmission at detached breakwaters for shoreline response modeling, Technical Note ERDC/CHL CHETN-II-45, Vicksburg, Mississippi, U.S. Army Engineer Research and Development Center, Coastal and Hydraulics Laboratory, 2002.

Wang, H., Darlymple, R. A. and Shiau, J. C.: Computer simulation of beach erosion and profile modification due to waves, Proc. 2nd Annaul Symp. Waterways, Harbours and Coastal Engrg. Div., ASCE, 1975.

https://doi.org/10.5194/nhess-2023-166
Preprint. Discussion started: 18 October 2023

Yates, M. L., Guza, R. T., O'Reilly, W. C.: Equilibrium shoreline response: Observations and modeling, J. Geophysical Research: Oceans, 114, https://doi.org/10.1029/2009JC005359, 2009.

Yu, J. T. and Chen, Z. S.: Study on headland-bay sandy stability South China coasts, China Ocean Engineering, 25, 1, 1–13. 2011.

460